



OPEN Warm, not cold temperatures contributed to a Late Miocene reef decline in the Coral Sea

Benjamin Petrick¹✉, Lars Reuning¹, Gerald Auer², Yige Zhang³, Miriam Pfeiffer¹ & Lorenz Schwark¹

Evidence shows that in the modern ocean, coral reefs are disappearing, and these losses are tied to climate change. However, research also shows that coral reefs can adapt rapidly to changing conditions leading some researchers to suggest that some reef systems will survive future climate change through adaptation. It is known that there were changes in the area covered by coral reefs in the past. Therefore, it is important to investigate the long-term response of coral reefs to environmental changes and high sea-surface temperatures (SSTs). However, because of diagenetic issues with SST proxies in neritic, metastable carbonate-rich environments, there is an incomplete and sometimes even incorrect understanding of how changes in SSTs affect carbonate reef systems. A good example is the Queensland Plateau offshore northeast Australia next to the threatened Great Barrier Reef. In the Late Miocene, between 11 and 7 Ma, a partial drowning caused the reef area on the Queensland Plateau to decline by ~50% leading to a Late Miocene change in platform geometry from a reef rimmed platform to a carbonate ramp. This reef decline was interpreted to be the result of SSTs at the lower limit of the modern reef growth window (20–18 °C). This article presents a new Late Miocene—ased SST record from the Coral Sea based on the TEX₈₆^H molecular paleothermometer, challenging this long held view. Our new record indicates warm tropical SSTs (27–32 °C) at the upper end of the modern reef growth window. We suggest that the observed temperatures potentially exceeded the optimal calcification temperatures of corals. In combination with a low aragonite supersaturation in the ocean, this could have reduced coral growth rates and ultimately lowered the aggradation potential of the reef system. These sub-optimal growth rates could have made the coral reefs more susceptible to other stressors, such as relative sea-level rise and/or changes in currents leading to reef drowning. Given that these changes affected coral reefs that were likely adapted to high temperature/low aragonite saturation conditions suggests that reefs that have adapted to non-ideal conditions may still be susceptible to future climate changes due to the interaction of multiple stressors associated with climate change.

According to the Intergovernmental Panel on Climate Change, coral reefs are considered to be one of the most susceptible environments to future climate change¹. Corals provide key ecosystem services and are the highest economic value environment due to a combination of benefits for tourism, fishing, and coastal protection, among other benefits^{2,3}. However, many of these reef systems are impacted by modern climate change¹. This is true of the Australian Great Barrier Reef (GBR), which has shown repeated bleaching events over the last 10 years⁴. Yet at the same time, work from the Persian Gulf shows that corals can adapt to maximum monthly average SSTs around 34 °C in less than 6 ka^{5–7}. Other studies have suggested coral reef adaptations to other aspects of future climate change, including acidification and changing sea levels^{8–10}. This has led to a debate about the future of coral reefs between those who argue that adaptation will allow at least some reef systems to survive⁸ and those that argue that multiple stressors will lead to complete coral reef loss¹¹. Resolving this debate is difficult as coral reef systems normally develop and decline on geological time scales beyond direct human observation. Therefore, it is important to understand what caused coral reef loss in the past, especially during periods where SSTs were higher than today. However, our understanding of how climate changes influenced reef systems in the past is poor.

¹Institute of Geosciences, Christian-Albrechts-Universität zu Kiel, Ludewig-Meyn-Straße 10, 24118 Kiel, Germany. ²Institute of Earth Sciences, NAWI Graz Geocenter, University of Graz, Heinrichstrasse 26, 8010 Graz, Austria. ³Department of Oceanography, Texas A&M University, College Station, TX 77843, USA. ✉email: benjamin.petrick@ifg.uni-kiel.de

A key challenge is that many quantitative geochemical proxies do not work on and in the vicinity of carbonate platforms, especially on multi-million-year time scales. This is because of issues with carbonate diagenesis, low total organic matter content, and a lack of long drill cores from reefs. Therefore, even though the timing of the loss of coral reefs and degradation of carbonate platforms is known during periods of the past, tying these changes to climatic change has been difficult¹². This has led to a distorted view of the causes of coral loss in the past and our poor understanding of how changes in multiple environmental stressors affect coral reef systems and carbonate platforms over geological time scales.

The Queensland Plateau forms an isolated plateau offshore the GBR in the Coral Sea. Today it hosts several small pinnacle reefs and larger reef complexes, which together occupy 10–15% of its surface¹³. The modern reefs are relics of an Early to Middle Miocene (20–11 Ma) reef rimmed platform which covered ~64,000 km²¹⁴. In the Late Miocene, between 11 and 7 Ma, a partial drowning resulted in a decline of the reef area by 50%¹⁵. This change was accompanied by a shift in platform geometry from a reef-rimmed platform to a carbonate ramp during the Late Miocene¹⁶.

The Late Miocene has been suggested to be a time where average SSTs were similar to future climate change predicted for the end-of-century scenarios¹⁷. However, despite this, cool surface temperatures have been suggested as a reason for this dramatic reef decline, combined with other stressors such as changes in sea level and erosion^{14, 15, 18, 19}. This interpretation is based on a $\delta^{18}\text{O}_{\text{Globigerinoides ruber}}$ SST-reconstruction from ODP Site 811 on the Queensland Plateau (Fig. 1)¹⁵, which suggests SSTs ranged from 18 to 20 °C during the Late Miocene. These SST values are at the lower limit of the temperature range that supports reef growth²⁰. Therefore, there is a disconnect between the high global SSTs and the temperatures reported from the Coral Sea during the Late Miocene. This study will re-evaluate the paleotemperature record from ODP site 811.

Studies using up-to-date methods have found temperatures at many other sites to be warmer than the original $\delta^{18}\text{O}$ SST reconstructions indicated^{26, 27}. Detailed studies found that $\delta^{18}\text{O}$ SST estimates were about 10 °C too cold for Miocene tropical environments when using non-glassy foraminifera due to the alteration of their calcitic tests²⁸. An alkenone-based U^K_{37} SST record from the upper continental slope just offshore the GBR in the Coral Sea, showed a very different trend to a $\delta^{18}\text{O}$ glacial/interglacial record that was assumed to record SST²⁹. However, even when knowing that the original $\delta^{18}\text{O}$ records are problematic it remains a challenge to reconstruct SSTs in environments close to carbonate platforms that are rich in metastable carbonate phases with high diagenetic potential, such as aragonite. This is due to the influence of diagenetic phases in these environments, which can hamper the use of proxies such as $\delta^{18}\text{O}$, clumped isotopes, or Mg/Ca from carbonate archives^{12, 29, 30}. The use of alkenone-based proxies such as U^K_{37} is limited to sea surface temperature < 29 °C and is poor at recording SSTs above 27 °C³¹, a temperature that can be exceeded in a tropical environment typical for reef growth. Therefore, a new proxy is needed to test the impact of SSTs on coral reefs in the past.

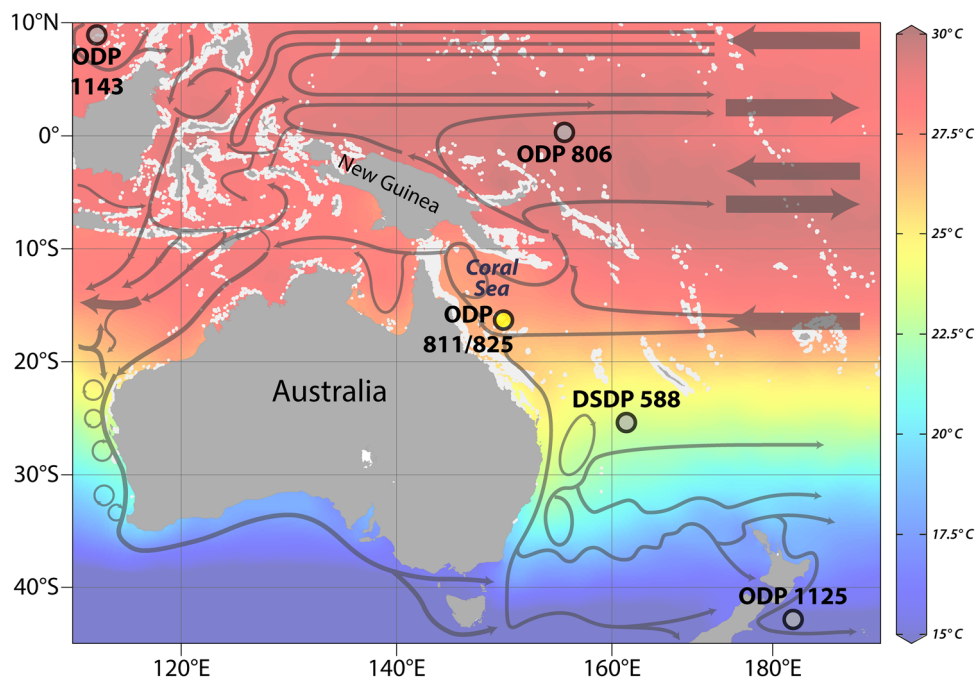


Figure 1. Location map of the Coral Sea and ODP Sites 811 and 825. Average sea surface temperatures (in °C) are based on the World Ocean Atlas 2018 (WOA18) annual mean temperature data, which is averaged from 1955 to 2010²¹. The SST color map was generated together with the base map in the program Ocean Data View²². The distribution of coral reefs, shown in white, is based on the dataset available from UN Environment Programme World Conservation Monitoring Centre²³. Currents are simplified from²⁴ and were adapted from²⁵.

TEX₈₆-based reconstructions can provide a better estimate of SST in these diagenetically active, metastable carbonate-rich environments. This is because TEX₈₆ is based on the lipid composition of membranes from Thaumarchaeota found in many different parts of the ocean, and has been found including in low-productivity environments³². Because TEX₈₆ is based on lipid biomarkers from a non-calcite organism, it is not susceptible to carbonate alteration or dissolution like other SST proxies³³. Also, TEX₈₆ is one of the few biomarker indexes that record temperatures above 30 °C, which is vital for reconstructing SSTs in tropical environments³⁴. The biggest issue in the past has been the typically low organic matter content values in periplatform settings and questions about the accuracy of TEX₈₆. However, large sample sizes, new, more sensitive methodologies, and a better understanding of the depth of production for TEX₈₆ data have improved these issues (See supplement Sect. 1 for more info). Therefore, TEX₈₆ provides a unique opportunity to reevaluate whether the extensive coral reef system of the Queensland Plateau was lost due to cooling between 11 and 7 Ma when studies suggest the platform drowned¹⁵.

ODP Site 811 (Fig. 1) was chosen for this project because it provides a continuous record of climate change from the Queensland Plateau for the last 11 Ma, as highlighted by our updated and improved age model (Fig. 2). We produced a new TEX₈₆H-based biomarker SST record for ODP Site 811 from 11 to 7 Ma.

Results and discussion

Results. The TEX₈₆^H derived SSTs at ODP Site 811, range from 32 to 27 °C, and were 9–12 °C warmer in the late Miocene than the δ¹⁸O-based SSTs previously published (Fig. 3). Based on running averages, there is no cooling or warming trend in the data overall (Fig. 3). The combined method and instrumental error of TEX₈₆^H is 3 °C for each analysis, which, even at its maximum, does not encompass the old data. For data quality assurance, we ran several tests to determine if the TEX₈₆ was influenced by non-thermal sources such as the Methane Index³⁵ and Ring Index³⁶ or affected by outside sources using tests such as the BIT index³⁷. Our work shows little evidence for a non-thermal input to the site. The BIT index is close to the quality threshold at the upper end of the section, but this only affects three data points. Overall, the tests show that the TEX₈₆ at this site is being produced in optimal conditions for SST analysis and do not explain the difference between TEX₈₆ and δ¹⁸O reconstructed temperatures. For a more detailed analysis of the TEX₈₆, please see supplemental Sect. 1. Average TEX₈₆^H-reconstructed SSTs were 29.7 °C, compared to the original δ¹⁸O-based SST average value of 20.8 °C¹⁵.

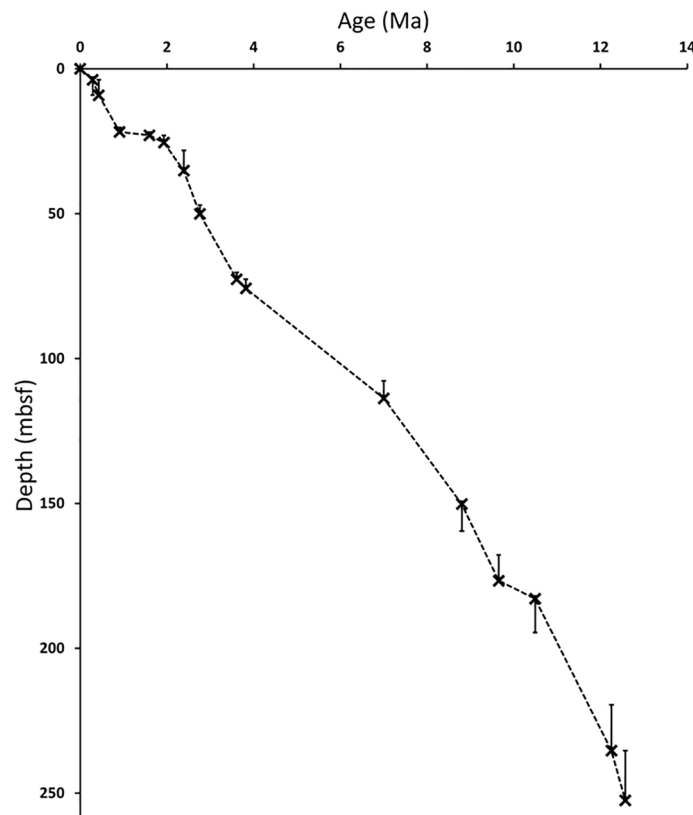


Figure 2. Age-depth model of ODP Site 811. Biostratigraphic markers are indicated as black crosses with potential depth errors shown as whiskers. Base occurrences are generally assumed to only have a positive depth (= deeper core depth) error while Top occurrences can only have a negative depth (= shallower core depths) error (see Tab. 1). Due to the nature of the last and first occurrences in the stratigraphic record.

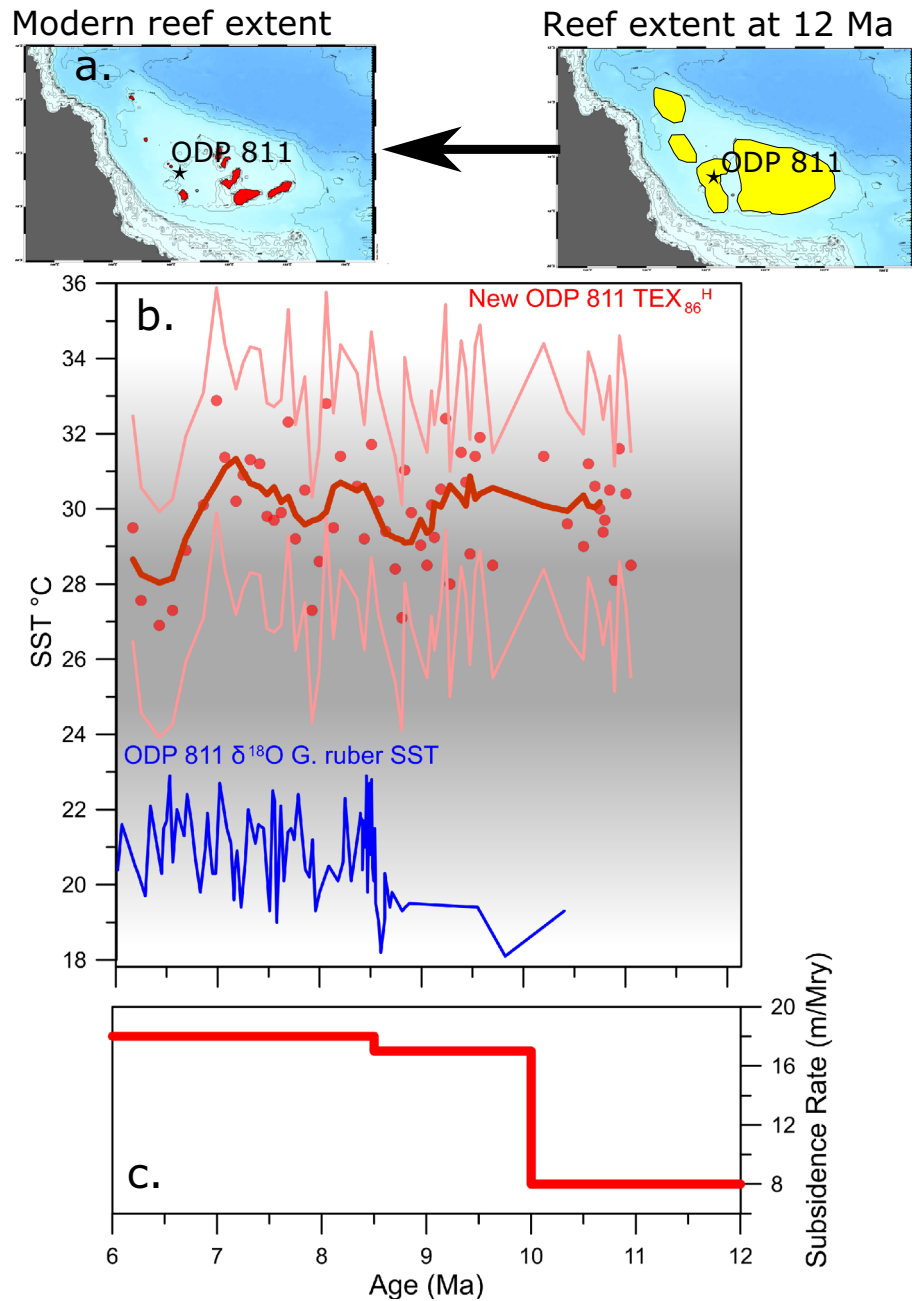


Figure 3. (a) maps of reefs before the late Miocene loss and the modern reef system on the Queensland Plateau based on reconstructions from^{14, 15} (b) New $\text{TEX}_{86}^{\text{H}}$ SST (red) and the previous *G. ruber* $\delta^{18}\text{O}$ derived SST (blue)¹⁵. The raw data from the new $\text{TEX}_{86}^{\text{H}}$ record is shown by red dots, and a 7-point running average is shown by the thick red line. The 2-sigma error of the $\text{TEX}_{86}^{\text{H}}$ proxy is shown by the light pink lines. The temperature range of the modern “reef growth window” is shown in darker gray⁴¹. (c) Subsidence rates (red line) from⁴² for ODP Site 1193 on the Marion Plateau in the Coral Sea.

Regional SST comparisons. The $\text{TEX}_{86}^{\text{H}}$ SSTs are close to the average SSTs of 29.9 °C from ODP 806 in the modern West Pacific Warm Pool over the same time interval (Figs. 1, 4). Comparing our record to other SST records from sites in the western Pacific warm pool, based on $\text{TEX}_{86}^{\text{H}}$ (Fig. 4) shows that the temperatures and trends are very similar to those seen in the West Pacific Warm Pool during the Late Miocene³¹ (Fig. 4).

They are slightly warmer than $\text{TEX}_{86}^{\text{H}}$ temperatures from DSDP site 588 south of the site at the southernmost limit of the Coral Sea at the Lord Howe Rise. Together with being slightly cooler than the sites further north suggests that the SSTs from ODP site 811 fall within the expected SST gradient³⁸. However, the ODP site 811 SSTs we found are very different from the SSTs and cooling trends that were seen in most of the subtropical southern hemisphere during the Late Miocene³⁹ (Fig. 4). The original $\delta^{18}\text{O}$ SSTs are lower than the U^{K}_{37} temperatures at ODP site 1125 located just off of New Zealand on Tasman Front during this time further suggesting that these

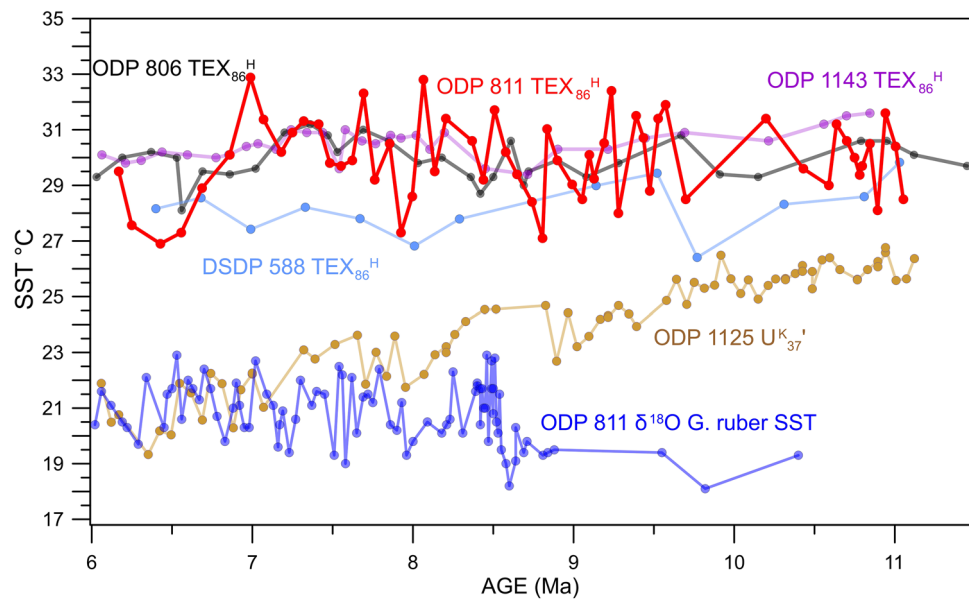


Figure 4. A comparison of different SST records from the western Pacific. The new 811 $\text{TEX}_{86}^{\text{H}}$ records from ODP site 811 (red) and the old $\delta^{18}\text{O}$ record¹⁵ are compared to other Sites from the western Pacific (Fig. 1). These include ODP site 806 from the WPWP to the north of the Coral Sea (black), ODP site 1143 from the southern South China Sea (purple)³¹, and DSDP site 588 from the Lord Howe Rise at the southern limit of the Coral Sea (light blue)³⁸ all of which are $\text{TEX}_{86}^{\text{H}}$ records. ODP site 1125 east of New Zealand south of the Tasman front (gold)³⁹ is a U^{K}_{37} record. See Fig. 1 for locations of sites.

SSTs do not fit with other SST reconstructions for this time³⁹ (Fig. 4). This suggests that the Coral Sea was tropical rather than subtropical, as previously suggested¹⁵, during the Late Miocene. Given that the average SST at the Coral Sea today is between 24 and 25 °C²¹ (Fig. 1), Late Miocene temperatures were between 2 and 6 °C warmer than in the modern Coral Sea. During the Late Miocene, the site was only 3 degrees further south⁴⁰, meaning that latitudinal drift would not explain the changes.

The $\text{TEX}_{86}^{\text{H}}$ SSTs are 9–12 °C warmer than the old $\delta^{18}\text{O}$ SST record. Research showed that when “frosty” foraminifera showing authigenic calcite overgrowth, as opposed to glassy foraminifera, are used, the reconstructed $\delta^{18}\text{O}$ temperatures are about 10 °C too cold²⁷. This recrystallization is produced in the deep ocean and adds a benthic temperature component on top of the SST signature preserved in the test, causing the cold bias. The initial reports describe overgrowths and infillings as minimal¹⁸. While this would have been seen as well preserved at the time of publication, today, these foraminifera would be described as frosty, which is defined as foraminifera that has undergone relatively modest diagenetic alteration²⁷. The presence of overgrowth has been confirmed by re-examining the foraminifera as part of this study. Therefore, despite the best attempts to avoid overgrowth effects, they are affecting the $\delta^{18}\text{O}$ record. However, the inferred Late Miocene cooling and its effect on the reefs of the Queensland Plateau were not just based on the $\delta^{18}\text{O}$ -SSTs but were supported by carbonate facies analysis.

Re-analysis of carbonate facies. The reduction in coral reef platform area in the late Miocene was accompanied by a transition in carbonate platform morphology and biota on the analyzed southwestern margin of the Queensland Plateau¹⁶. The Middle Miocene rimmed carbonate platform was dominated by a tropical photozoan skeletal assemblage, including green algae, corals, and large benthic foraminifera. Bryozoans occur as a minor component. During the Late Miocene, the platform evolved into a carbonate ramp with a skeletal assemblage dominated by bryozoans and foraminifera, including abundant large benthic foraminifera but also planktonic foraminifera¹⁶. In contrast, corals and green algae are missing in these upper Miocene deposits. It was thought that the Late Miocene facies is more representative of a foramol association (sensu⁴³)¹⁶. This shift in the skeletal assemblage was interpreted to reflect a transition from tropical to non-tropical, warm-temperate climate conditions^{14–16, 18}, partly supported by the oxygen isotope record^{15, 18}.

Additionally, a number of researchers¹⁵ have discussed the possibility that changes in nutrients influenced the facies transition on the Queensland Plateau. Based on paleontological data it was thought that an increased nutrient availability would have contributed to the Late Miocene facies transition¹⁵. Others in contrast argued that an influence of nutrients would be unlikely, partly based on the fact that large benthic foraminifera assemblages in mesotrophic environments typically would be rich in large imperforate forms while the Late Miocene carbonates from the Queensland Plateau are characterized by perforated forms¹⁶. However, it has been shown that perforate large benthic foraminifera are common in Miocene equatorial carbonates with foramol facies⁴⁴. These carbonates were deposited under tropical temperatures where nutrient levels were in the high oligotrophy to mesotrophy range⁴⁴. There is now a growing number of studies demonstrating that carbonate platforms

dominated by foramol and other heterozoan skeletal grain associations were thriving under tropical temperature conditions during the Miocene^{45–47}. All of these studies emphasized that carbonate grain associations on their own are insufficient to allow an unequivocal interpretation of paleoclimatic conditions. It has been stressed that other data, e.g. from climate proxy studies, are required to support an environmental interpretation⁴⁸. Our presented new temperature proxy data presented here shows that environmental factors other than temperature are responsible for the observed carbonate facies change on the Queensland Plateau during the Miocene. A more detailed assessment of the paleontological and facies evidence for sea surface temperature conditions is given in the supplemental "Results and discussion" section.

Implications for coral reef development. Our new $\text{TEX}_{86}^{\text{H}}$ SST data suggests a new driver is needed to explain the loss of corals. We find it is unlikely that cooler SSTs were responsible for the loss of these reefs, as suggested in the classical study of Isern et al.¹⁵. Our $\text{TEX}_{86}^{\text{H}}$ SST data fall within the upper end of the modern "reef growth window" during the time of the coral reef drowning, which defines the environmental conditions that are optimal for the development of reefs⁴¹. SSTs between 25° and 29 °C generally are considered to be ideal for reef development⁴¹, while winter temperatures of 18 °C define the lower limit²⁰ (Fig. 3). An upper-temperature limit for modern reef growth is not well defined, but coral reefs in the Persian Gulf experience annual average temperatures of ~28 °C SST, but with summer temperatures exceeding 34 °C^{5,20}. Generally, the calcification and upward growth rates of many coral species increase linearly with annual SST^{49,50}. However, this trend seems to reverse above an annual temperature of 26–27 °C, with a reduction of the calcification and extension rate at higher temperatures⁵¹. There is pronounced taxonomic variation in the effect of temperature on corals, but a recent meta-analysis indicates that severe future temperature increases are expected to reduce their calcification rates and therefore could limit their capacity to build reefs⁵². Hence the observed Late Miocene average temperatures of ~30 °C (Fig. 3) might have induced stressed conditions in the coral reefs of the Queensland Plateau during the Late Miocene similar to what is occurring in the GBR in the modern-day.

Additionally, there might have been limited coral calcification and extension rates due to the relatively low aragonite supersaturation in the Mid-Late Miocene tropical ocean. Reconstructions indicate that the aragonite supersaturation in the tropical ocean was lower in the Late Miocene compared to pre-industrial values, with a minimum at ~9Ma⁵³. This is similar to the modern ocean where acidification is predicted to impact future coral reef net carbonate production. It was observed that the calcification rate of reef corals was lower than present-day values for much of the Neogene, not only in marginal basins but also in examples from clear-water reef window-type environments⁵⁴. This change is explained with the chronically low carbonate saturation state of the global ocean during this time. Therefore, much like in the modern ocean, the Late Miocene corals were experiencing high thermal conditions and low aragonite supersaturation. Environmental conditions such as temperature and aragonite supersaturation impact the rates of coral reef carbonate production and their capacity to accrete to sea level in many ways⁵⁵. Bioerosion and synsedimentary carbonate dissolution are other important factors besides coral calcification rates. The response of coral reef net carbonate production to changes in temperature and aragonite saturation state is complex⁵⁵. However, lower aragonite saturation states are not only expected to reduce coral calcification rates⁵² but also to increase bioerosion⁵⁶ and reef carbonate dissolution⁵⁷.

Yet despite these conditions, this did not lead to coral reef loss in the Coral Sea, and there is some evidence that the corals had adapted to the suboptimal conditions by 11 Ma. During the Mid-Miocene Climatic Optimum (MMCO), tropical ocean temperatures likely were similar to, or higher than SSTs during the late Miocene^{58–60}, and the surface ocean aragonite saturation state was even lower compared to the Late Miocene⁵⁴. Despite this, reef growth was abundant and even showed signs of expansion on the Queensland Plateau during the MMCO¹⁶. The corals that existed during the Late Miocene, as mentioned above, may have adapted to these MMCO conditions. This is similar to the modern where coral reefs can adapt to grow in suboptimal environments such as the Persian Gulf^{6–7}. However, despite these adaptations, the coral reefs still declined between 11 and 7 Ma. Therefore, while warm SSTs and low aragonite saturation might have reduced net reef carbonate production, we believe that this alone could not have caused the dramatic loss of coral reefs.

Therefore, our study suggests that additional changes must have triggered the collapse of an adapted coral reef system. There are two main candidates for this: increased subsidence or changes in ocean circulation. Increased subsidence could have contributed to the drowning of the coral reefs in the Coral Sea⁴². Research showed an increase in subsidence on the Marion Plateau just south of the Queensland Plateau between 11 and 10 Ma, concurrent with the loss of the coral reefs. This was matched by high late Neogene subsidence rates seen on the NW shelf of Australia^{61,62}. Therefore, there is some evidence for increased subsidence rates over large parts of the northern Australian plate around 11 Ma. However, the subsidence rates were insufficient to outpace the aggradation potential of modern coral reefs⁴². Therefore, the combined effects of high subsidence rates, the lower aragonite supersaturation during the Late Miocene, and the higher SSTs we found in this study could have put the coral reefs at risk. This would have meant that the coral reefs were not able to keep up with the change to higher subsidence rates at around 10 Ma. Therefore, this event could have caused the coral reefs, which had adapted to high SSTs by reducing extension rates to drown.

An additional stressor could have been the intensification of open ocean currents during between 12 and 8 Ma⁶³, which could have aggravated the Late Miocene coral reef demise in the Coral Sea¹⁹. There is evidence of shifting wind and current patterns during the late Miocene^{63,64}. It was hypothesized that cooler late Miocene SSTs at the Queensland Plateau could indicate an increased influence of southern sourced waters and intensification of the sub-thermocline water mixing¹⁵. This does not fit our SST record, and we do not see any evidence for long-term permanent SST cooling during 11 to 7 Ma when the coral reefs drowned (Figs. 2, 3) as would be expected with a change in currents. Even the coldest temperatures reconstructed at Site 811 are still in the

Nannofossil event	Age (Ma)	Depth (mbsf)	Depth error (mbsf)	Site	Reference
B. <i>Emiliana huxleyi</i>	0.29	3.82	5.32	ODP 811	Gradstein et al. ⁷⁰
T <i>Pseudoemiliana lacunosa</i>	0.43	9.13	5.32	ODP 811	Gradstein et al. ⁷⁰
T <i>Reticulofenestra asanoi</i>	0.91	21.82	1.52	ODP 811	Gradstein et al. ⁷⁰
T <i>Calcidiscus macintyreii</i>	1.60	22.99	1.18	ODP 811	Gradstein et al. ⁷⁰
T <i>Discoaster brouweri</i>	1.93	25.49	2.5	ODP 811	Gradstein et al. ⁷⁰
T <i>Discoaster pentaradiatus</i>	2.39	35.18	7.04	ODP 811	Gradstein et al. ⁷⁰
T <i>Discoaster tamalis</i>	2.76	50.10	3.02	ODP 811	Gradstein et al. ⁷⁰
T <i>Sphenolithus spp.</i>	3.61	72.63	2.38	ODP 811	Gradstein et al. ⁷⁰
T <i>Reticulofenestra pseudoumbilicus</i>	3.82	75.79	3.16	ODP 811	Gradstein et al. ⁷⁰
Ta <i>Reticulofenestra pseudoumbilicus</i>	7.10	113.79	6.12	ODP 811	Gradstein et al. ⁷⁰
Ba <i>Reticulofenestra pseudoumbilicus</i>	8.80	150.26	9.37	ODP 811	Gradstein et al. ⁷⁰
T <i>Discoaster hamatus</i>	9.61	176.7	8.9	ODP 811	Gradstein et al. ⁷⁰
B <i>Discoaster hamatus</i>	10.57	182.9	11.66	ODP 811	Gradstein et al. ⁷⁰
T <i>Coronocyclus nitescens</i>	12.25	235.35	15.82	ODP 825	Gradstein et al. ⁷⁰
Tc <i>Calcidiscus premacintyreii</i>	12.57	252.48	17.13	ODP 825	Gradstein et al. ⁷⁰

Table 1. Nannofossil biostratigraphic events detected during the semiquantitative screening of 53 samples (see supplementary material nannofossil data and depth uncertainty of the datums). Ages are based on the most recent compilation in the Geologic Time Scale 2020⁷⁰. B Base occurrence, T Top occurrence; Ba Base absence; Ta Top absence; Tc Top common cf.^{71, 72}.

tropical “coral reef window” (Figs. 2, 3). This observation is consistent with the limited data from the southern limit of the Coral Sea at ODP 588³⁸.

It was suggested that a new wind-driven current system was established in the Coral Sea during the Late Miocene¹⁹. They argue that this could have caused topographical mixing and upwelling of nutrient-rich subsurface waters on the leeward side of the Queensland Plateau, ultimately causing the backstepping of the leeward margin and the reduction in platform size. Additionally, they emphasize that strong current systems can have detrimental effects on carbonate platforms, e.g. through intensified erosion limiting their potential to aggrade and keep up with sea-level rise¹⁹. Therefore, whichever combination of stressors, it seems that synergetic stressors might explain the reduction in reef area in the Coral Sea during the Late Miocene.

In summary, our work shows that the long-held hypothesis that the Late Miocene carbonate platform drowning in the Coral Sea was caused by cooling must be revised. SSTs remained warm and even exceeded the optimal temperature range of modern coral reef growth during the entire period. Instead, we suggest that SSTs on the higher end of the modern reef growth window and the relatively low aragonite saturation state of the surface ocean made the coral reef more susceptible to other environmental stressors, such as the relative sea-level rise and increased erosion, and/or nutrient inputs from open ocean currents. The combination of stressors likely led to the partial drowning of the Queensland Plateau between 11 and 7 Ma.

Interestingly, these drivers are similar to those predicted for future climate change. Models show that SSTs and sea levels will increase with future climate change⁶⁵. Furthermore, high CO₂ levels are leading to increased acidification of the oceans, inhibiting carbonate production⁶⁵. It may be that the coral reefs on the Queensland Plateau had successfully adapted to the climate changes experienced during the Mid-Miocene. However, these adaptations might have left the corals susceptible to changes in sea level and possibly changing nutrient conditions. Model studies show that modern coral reefs could survive various individual climate change effects either through adaptation or by migration to more protected environments⁵⁵. However, combining the various stressors into a single model significantly reduces the survivability of coral reefs⁵⁵. Our record shows that in combination with other factors, high SSTs can cause a significant decline of coral reefs with a similar set of conditions as predicted by models issued by the International Panel on Climate Change⁵⁵. Therefore, our record shows that the loss of coral reefs in the Coral Sea during the Late Miocene was not a result of rapid cooling in SSTs but instead a combination of negative stresses that together lead to the observed dramatic reduction in reef area between 11 and 7 Ma.

Methods

Age model. The biostratigraphic age model of ODP Site 811/825 was reevaluated based on a semiquantitative study of 53 samples from the entire core including sections outside of the SST reconstructions done above (see supplementary data for details). Slides were prepared according to the drop technique (cf.⁶⁶; see⁶⁷ for details on the methodology). Samples were screened for nannofossils and their presence was recorded based on a distinction between few (F: one to five specimens per slide), rare (R: one specimen every other field view), common (C: one to five specimens per field view), abundant (A: more than 10 specimens per field view), and dominant (D: taxon occurs ubiquitously with only rare occurrence of other taxa present). The maximum potential depth error of the recorded nannofossil datums results from sample spacing between the unequivocal record of a taxon and its absence in the next sample above (for top occurrences: T), or below (for base occurrences: B). In the

age-depth plot (Fig. 2), this uncertainty is also expressed as vertical error bars^{68,69}. The defined biostratigraphic events are summarized in Table 1 and the age-depth model is visualized in Fig. 4.

GDGTs. For this project, we took 50 cc of sediment leading to between 50 and 60 g of sediment being extracted. Pilot work showed that this was necessary to have enough material to measure SSTs on. Samples were Soxhlet extracted for 48 h using a solvent mixture of DCM: MeOH (9:1, v/v). Elemental sulfur was removed by the addition of activated copper turnings. Excess solvent was evaporated by a Büchi solvent evaporator to a final volume of 2 ml and samples were then transferred into a 4 ml vial, where the total extract (TE) was taken to dryness under a gentle stream of nitrogen. TEs were fractionated into aliphatic, aromatic, and polar fractions by silica gel-column chromatography (6 ml SPE column, 2.8 g Silica 60 mesh, 25–40 µm) using solvents with increasing polarity in an LC-TECH automated SPE system. NSO (polar) compounds were eluted with 14 ml DCM/ MeOH (1:1, v/v). The polar fraction was reconstituted in hexane/isopropanol (9:1, v/v) and re-chromatographed over aminopropyl-substituted silica gel (3 ml SPE column, 1.0 g aminopropyl-silica, 25–40 µm). The alcohol fraction containing the GDGTs was eluted with 5 ml of hexane/isopropanol (9:1, v/v) and after drying was re-dissolved in hexane/isopropanol (99:1, v/v) to a final concentration of 6 mg/ml for injection into the HPLC/MS system.

GDGTs were measured on an Alliance 2695 HPLC system (Waters, UK) coupled to a Micromass ZQ single quadrupole mass spectrometer following the analytical protocol of⁷³. The HPLC instrument was equipped with two Waters BEH HILIC silica columns (2.1 × 150 mm; 1.7 µm particle size) and a guard column maintained at 30 °C. Target compounds were eluted with a flow rate of 0.2 ml/min starting isocratically with 82% eluent A (n-hexane) and 18% eluent B (n-hexane:2-propanol (9:1, v/v)) for 25 min. Thereafter, a linear gradient was set to 65% eluent A and 35% eluent B in 25 min, followed by a linear gradient to 0% eluent A and 100% eluent B in 30 min. Re-equilibration of the column afforded 82% eluent A and 18% eluent B for 20 min. Detection of isoprenoid GDGTs was achieved using a Micromass ZQ single quadrupole mass spectrometer (MS) equipped with an atmospheric pressure chemical ionization (APCI) interface operated in positive ion mode. MS settings were: source temperature, 150 °C; vaporizer temperature, 500 °C; corona, 2 µA; cone voltage, 40 V; extractor voltage, 3 V; radio frequency (RF) lens, 0.1 V; desolvation gas, N₂ at 8 L/min. Detection of archaeal core lipids was achieved by single ion recording of their protonated molecular ions [M + H]⁺ (dwell time, 234 ms) and compounds were quantified by integration of peak areas using MassLynx© software. Calculation of TEX₈₆ followed⁷⁴ and TEX₈₆^H followed³⁴. Reproducibility upon duplicate measurements showed a relative standard error of < 2% and samples analyzed using both methods showed a relative standard error of < 3%.

Data availability

All data needed to evaluate the conclusions in the paper are present in the paper and/or the Supplementary Materials. The datasets used and/or analyzed during the current study will be available from the corresponding author upon reasonable request. Requests for the data should be submitted to: benjamin.petrick@ifg.uni-kiel.de.

Received: 6 October 2022; Accepted: 6 March 2023

Published online: 10 March 2023

References

- Pörtner, H.-O. *et al.* The ocean and cryosphere in a changing climate. (2019).
- de Groot, R. *et al.* Global estimates of the value of ecosystems and their services in monetary units. *Ecosyst. Serv.* **1**, 50–61 (2012).
- Pendleton, L. *et al.* Coral reefs and people in a high-CO₂ World: Where can science make a difference to people?. *PLoS ONE* **11**, e0164699 (2016).
- Great Barrier Reef Marine Park Authority, Australian Institute of Marine Science & CSIRO. *Reef snapshot: summer 2021–22*. <https://library.gbrmpa.gov.au/jspui/handle/11017/3916> (2022).
- Howells, E. J. *et al.* Species-specific coral calcification responses to the extreme environment of the southern Persian Gulf. *Front. Mar. Sci.* **4**, 56 (2018).
- Kirk, N. L., Howells, E. J., Abrego, D., Burt, J. A. & Meyer, E. Genomic and transcriptomic signals of thermal tolerance in heat-tolerant corals (*Platygyra daedalea*) of the Arabian/Persian Gulf. *Mol. Ecol.* **27**, 5180–5194 (2018).
- Smith, E. G. *et al.* Signatures of selection underpinning rapid coral adaptation to the world's warmest reefs. *Sci. Adv.* **8**, 7287 (2022).
- Rinkevich, B. Coral chimerism as an evolutionary rescue mechanism to mitigate global climate change impacts. *Glob. Chang. Biol.* **25**, 1198–1206 (2019).
- Kubicek, A., Breckling, B., Hoegh-Guldberg, O. & Reuter, H. Climate change drives trait-shifts in coral reef communities. *Sci. Rep.* **9**(1), 1–10 (2019).
- Ritson-Williams, R. & Gates, R. D. Coral community resilience to successive years of bleaching in Kāneʻohe Bay, Hawaiʻi. *Coral Reefs* **39**, 757–769 (2020).
- Gunderson, A. R., Tsukimura, B. & Stillman, J. H. indirect effects of global change: From physiological and behavioral mechanisms to ecological consequences. *Integr. Comp. Biol.* **57**, 48–54 (2017).
- Reuning, L., Reijmer, J. J. G., Betzler, C., Swart, P. & Bauch, T. The use of paleoceanographic proxies in carbonate periplatform settings—Opportunities and pitfalls. *Sediment. Geol.* **175**, 131–152 (2005).
- Davies, P. J., Symonds, P. A., Feary, D. A. & Pigram, C. J. The evolution of the carbonate platforms of Northeast Australia. *Control Carbonate Platf. Basin Dev.* <https://doi.org/10.2110/PEC.89.44.0233> (1989).
- Betzler, C., Brachert, T. C. & Kroon, D. Role of climate in partial drowning of the Queensland Plateau carbonate platform (North-eastern Australia). *Mar. Geol.* **123**, 11–32 (1995).
- Isern, A. R., McKenzie, J. A. & Feary, D. A. The role of sea-surface temperature as a control on carbonate platform development in the western Coral Sea. *Palaeoogeogr. Palaeoecol. Palaeoecol.* **124**, 247–272 (1996).
- Betzler, C. Ecological controls on geometries of carbonate platforms: Miocene/Pliocene shallow-water Microfaunas and carbonate biofacies from the Queensland Plateau (NE Australia). *Facies* **37**, 147–166 (1997).
- Steinthorsdottir, M. *et al.* The Miocene: The future of the past. *Paleoceanogr. Paleoclimatol.* **36**, e2020PA004037 (2021).
- Isern, A. R., McKenzie, J. A. & Müller, D. W. Paleocene changes and reef growth off the Northeastern Australian margin: Stable isotopic data from ODP Leg 133 Sites 811 and 817 and DSDP Leg 21 Site 209. *Proc. Ocean Drill. Program, 133 Sci. Results* doi:<https://doi.org/10.2973/ODP.PROC.SR.133.230.1993> (1993).

19. Betzler, C. & Eberli, G. P. Miocene start of modern carbonate platforms. *Geology* **47**, 771–775 (2019).
20. Kleypas, J. A., McManus, J. W. & Meñez, L. A. B. Environmental limits to coral reef development: Where do we draw the line?. *Am. Zool.* **39**, 146–159 (1999).
21. Boyer, T. P. *et al.* World Ocean Atlas 2018. *OAA National Centers for Environmental Information. Dataset.* (2018).
22. Schlitzer, R. Ocean data view. (2021) Retrieved from <https://odv.awi.de> ODV: ODV <https://odv.awi.de>.
23. UNEP-WCMC, WorldFishCentre & WRI, & T. Global distribution of warm-water coral reefs, compiled from multiple sources including the Millennium Coral Reef Mapping Project. Version 4.1. Includes contributions from IMaRS-USF and IRD (2005), IMaRS-USF (2005) and Spalding *et al.* (2001). *Cambridge (UK): UN Environment World Conservation Monitoring Centre.* doi:<https://doi.org/10.34892/t2wk-5t34>.
24. Wijeratne, S., Pattiaratchi, C. & Proctor, R. Estimates of surface and subsurface boundary current transport around Australia. *J. Geophys. Res. Ocean.* **123**, 3444–3466 (2018).
25. Auer, G. *et al.* Intensified organic carbon burial on the Australian shelf after the Middle Pleistocene transition. *Quat. Sci. Rev.* **262**, 106965 (2021).
26. Pearson, P. N. *et al.* Stable warm tropical climate through the Eocene Epoch. *Geology* **35**, 211–214 (2007).
27. Sexton, P. F., Wilson, P. A. & Pearson, P. N. Microstructural and geochemical perspectives on planktic foraminiferal preservation: “Glassy” versus “Frosty”. *Geochemistry. Geophys. Geosystems* **7**, n/a–n/a (2006).
28. Stewart, D. R. M., Pearson, P. N., Ditchfield, P. W. & Singano, J. M. Miocene tropical Indian Ocean temperatures: Evidence from three exceptionally preserved foraminiferal assemblages from Tanzania. *J. Afr. Earth Sci.* **40**, 173–189 (2004).
29. Lawrence, K. T. & Herbert, T. D. Late quaternary sea-surface temperatures in the western Coral Sea: Implications for the growth of the Australian great barrier reef. *Geology* **33**, 677–680 (2005).
30. Reuning, L., Reimer, J. J. G. & Mattioli, E. Aragonite cycles: Diagenesis caught in the act. *Sedimentology* **53**, 849–866 (2006).
31. Zhang, Y. G., Pagani, M. & Liu, Z. A 12-million-year temperature history of the tropical Pacific ocean. *Science* **344**, 84–87 (2014).
32. Damsté, J. S. S., Schouten, S., Hopmans, E. C., van Duijn, A. C. T. & Geenevasen, J. A. J. Crenarchaeol: The characteristic core glycerol dibiphytanyl glycerol tetraether membrane lipid of cosmopolitan pelagic crenarchaeota. *J. Lipid Res.* **43**, 1641–1651 (2002).
33. O’Connor, L. K. *et al.* Late Cretaceous temperature evolution of the southern high latitudes: A TEX₈₆ perspective. *Paleoceanogr. Paleoclimatol.* <https://doi.org/10.1029/2018PA003546> (2019).
34. Kim, J.-H. *et al.* New indices and calibrations derived from the distribution of crenarchaeal isoprenoid tetraetherlipids: Implications for past sea surface temperature reconstructions. *Geochemica Cosmochim. Acta* **74**, 4639–4654 (2010).
35. Zhang, Y. G. *et al.* Methane Index: A tetraether archaeal lipid biomarker indicator for detecting the instability of marine gas hydrates. *Earth Planet. Sci. Lett.* **307**, 525–534 (2011).
36. Zhang, Y. G., Pagani, M. & Wang, Z. Ring Index: A new strategy to evaluate the integrity of TEX₈₆ paleothermometry. *Paleoceanography* **31**, 220–232 (2016).
37. Hopmans, E. C. *et al.* A novel proxy for terrestrial organic matter in sediments based on branched and isoprenoid tetraether lipids. *Earth Planet. Sci. Lett.* **224**, 107–116 (2004).
38. Auderset, A. *et al.* Enhanced ocean oxygenation during Cenozoic warm periods. *Nature* **609**, 77–82 (2022).
39. Herbert, T. D. *et al.* Late Miocene global cooling and the rise of modern ecosystems. *Nat. Geosci.* **9**, 843–847 (2016).
40. Van Hinsbergen, D. J. J. *et al.* A paleolatitude calculator for paleoclimate studies. *PLoS ONE* **10**, e0126946 (2015).
41. James, N. P. & Bourque, P.-A. Reefs and mounds. in *Facies Models: Response to Sea Level Change* (eds. Walker, R. G. & James, N. P.) 323–347 (Geological Association of Canada, St. John’s, 1992).
42. DiCarpio, L. *et al.* A dynamic process for drowning carbonate reefs on the northeastern Australian margin. *Geology* **38**, 11–14 (2010).
43. Lees, A. & Buller, A. T. Modern temperate-water and warm-water shelf carbonate sediments contrasted. *Mar. Geol.* **13**, M67–M73 (1972).
44. Wilson, M. E. J. & Vecsei, A. The apparent paradox of abundant foramol facies in low latitudes: Their environmental significance and effect on platform development. *Earth Sci. Rev.* **69**, 133–168 (2005).
45. Bourrouilh-Le Jan, F. G. & Hottinger, L. C. Occurrence of rhodolites in the tropical Pacific—A consequence of Mid-Miocene paleo-oceanographic change. *Sediment. Geol.* **60**, 355–367 (1988).
46. Pomar, L., Brandano, M. & Westphal, H. Environmental factors influencing skeletal grain sediment associations: A critical review of Miocene examples from the western Mediterranean. *Sedimentology* **51**, 627–651 (2004).
47. Wilson, M. E. J. Global and regional influences on equatorial shallow-marine carbonates during the Cenozoic. *Palaeogeogr. Palaeoclimatol. Palaeoecol.* **265**, 262–274 (2008).
48. Westphal, H., Halfar, J. & Freiwald, A. Heterozoan carbonates in subtropical to tropical settings in the present and past. *Int. J. Earth Sci.* **99**, 153–169 (2010).
49. Brachert, T. C., Reuter, M., Kroeger, K. F. & Lough, J. M. Coral growth bands: A new and easy to use paleothermometer in paleoenvironment analysis and paleoceanography (late Miocene, Greece). *Paleoceanography* **21**, (2006).
50. Lough, J. M. & Cooper, T. F. New insights from coral growth band studies in an era of rapid environmental change. *Earth Sci. Rev.* **108**, 170–184 (2011).
51. Lough, J. M. & Cantin, N. E. Perspectives on massive coral growth rates in a changing ocean. *Biol. Bull.* **226**, 187–202 (2014).
52. Kornder, N. A., Riegl, B. M. & Figueiredo, J. Thresholds and drivers of coral calcification responses to climate change. *Glob. Chang. Biol.* **24**, 5084–5095 (2018).
53. Sosdian, S. M. *et al.* Constraining the evolution of Neogene ocean carbonate chemistry using the boron isotope pH proxy. *Earth Planet. Sci. Lett.* **498**, 362–376 (2018).
54. Brachert, T. C. *et al.* An assessment of reef coral calcification over the late Cenozoic. *Earth Sci. Rev.* **204**, 103154 (2020).
55. Cornwall, C. E. *et al.* Global declines in coral reef calcium carbonate production under ocean acidification and warming. *Proc. Natl. Acad. Sci. USA* **118**, e2015265118 (2021).
56. Schönberg, C. H. L., Fang, J. K. H. & Carballo, J. L. Bioeroding sponges and the future of coral reefs. *Clim. Chang. Ocean Acidif. Sponges Impacts Across Mult. Levels Organ.* 179–372 (2017) doi:https://doi.org/10.1007/978-3-319-59008-0_7/COVER/.
57. Eyre, B. D. *et al.* Coral reefs will transition to net dissolving before end of century. *Science* **359**, 908–911 (2018).
58. Sosdian, S. M. & Lear, C. H. Initiation of the western Pacific warm pool at the middle Miocene climate transition?. *Paleoceanogr. Paleoclimatol.* **35**, e2020PA003920 (2020).
59. Sosdian, S. M., Babila, T. L., Greenop, R., Foster, G. L. & Lear, C. H. Ocean carbon storage across the middle Miocene: A new interpretation for the Monterey event. *Nat. Commun.* **11**, 1–11 (2020).
60. Nairn, M. G., Lear, C. H., Sosdian, S. M., Bailey, T. R. & Beavington-Penney, S. Tropical sea surface temperatures following the middle Miocene climate transition from laser-ablation ICP-MS analysis of glassy foraminifera. *Paleoceanogr. Paleoclimatol.* **36**, e2020PA004165 (2021).
61. Belde, J., Back, S., Bourget, J. & Reuning, L. Oligocene and Miocene carbonate platform development in the Browse basin. *Aust. Northwest Shelf. J. Sediment. Res.* **87**, 795–816 (2017).
62. Rosleff-Soerensen, B., Reuning, L., Back, S. & Kukla, P. A. The response of a basin-scale Miocene barrier reef system to long-term, strong subsidence on a passive continental margin, Barcoo Sub-basin. *Aust. North West Shelf. Basin Res.* **28**, 103–123 (2016).
63. Groeneveld, J. *et al.* Australian shelf sediments reveal shifts in Miocene southern hemisphere westerlies. *Sci. Adv.* **3**, e1602567 (2017).

64. Bialik, O. M. *et al.* Monsoons, upwelling, and the deoxygenation of the Northwestern Indian ocean in response to middle to late miocene global climatic shifts. *Paleoceanogr. Paleoclimatol.* **35**, e2019PA003762 (2020).
65. Hoegh-Guldberg, O., Poloczanska, E. S., Skirving, W. & Dove, S. Coral reef ecosystems under climate change and ocean acidification. *Front. Mar. Sci.* **4**, 158 (2017).
66. Bordiga, M., Bartol, M. & Henderiks, J. Absolute nannofossil abundance estimates: Quantifying the pros and cons of different techniques. *Rev. Micropaléontologie* **58**, 155–165 (2015).
67. Auer, G. *et al.* Timing and pacing of Indonesian throughflow restriction and its connection to Late Pliocene climate shifts. *Paleoceanogr. Paleoclimatology* **34**, 635–657 (2019).
68. Auer, G., De Vleeschouwer, D. & Christensen, B. A. Toward a robust plio-pleistocene chronostratigraphy for odp site 762. *Geophys. Res. Lett.* **47**, e2019GL085198 (2020).
69. Del Gaudio, A. V., Piller, W. E., Auer, G. & Kurz, W. Integrated calcareous nannofossils and planktonic foraminifera biostratigraphy as tool to date serpentinite mud production for Fantangisña seamount on the Mariana forearc (IODP Expedition 366). *Newslett. Stratigr.* <https://doi.org/10.1127/NOS/2021/0673> (2021).
70. Gradstein, F. M. & Ogg, J. G. The chronostratigraphic scale. *Geol. Time Scale* **2020**, 21–32. <https://doi.org/10.1016/B978-0-12-824360-2.00002-4> (2020).
71. Backman, J., Raffi, I., Rio, D., Fornaciari, E. & Pálíke, H. Biozonation and biochronology of miocene through pleistocene calcareous nannofossils from low and middle latitudes. *Newslett. Stratigr.* **45**, 221–244 (2012).
72. Wade, B. S., Pearson, P. N., Berggren, W. A. & Pálíke, H. Review and revision of Cenozoic tropical planktonic foraminiferal biostratigraphy and calibration to the geomagnetic polarity and astronomical time scale. *Earth Sci. Rev.* **104**, 111–142 (2011).
73. Hopmans, E. C., Schouten, S. & Sinninghe Damsté, J. S. The effect of improved chromatography on GDGT-based palaeoproxies. *Org. Geochem.* **93**, 1–6. <https://doi.org/10.1016/j.orggeochem.2015.12.006> (2016).
74. Schouten, S., Hopmans, E. C., Schefuss, E., Sinninghe Damsté, J. S. & Damste, J. S. S. Distributional variations in marine crenarchaeotal membrane lipids: A new tool for reconstructing ancient sea water temperatures?. *Earth Planet. Sci. Lett.* **204**, 265–274 (2002).

Acknowledgements

The authors would like to thank the International Oceanic Discovery Program and the Kochi Institute for Core Sample Research for providing the samples used in this project. We would also like to thank all the participants of Expedition 133 for helping recover the samples. This project was funded with a grant from the Deutsche Forschungsgemeinschaft (DFG)—Project No. 447611930. The authors declare that they have no competing interests. Finally, I would like to thank Catherine Beltran and two anonymous reviewers who helped improve the manuscript in review.

Author contributions

All authors approved the manuscript and agreed to its submission. The corresponding author is B.P. All authors discussed the results and provided significant input to the final version of the manuscript. B.P. and L.R. designed the study. Y.Z. provided facilities to produce pilot data for the study. L.S. performed the biomarker analysis in his lab and interpreted data with B.P. G.A. provided a new-age model for the site. B.P., L.S., L.R., M.P., and G.A. provided vital feedback on the article.

Funding

Open Access funding enabled and organized by Projekt DEAL.

Competing interests

The authors declare no competing interests.

Additional information

Supplementary Information The online version contains supplementary material available at <https://doi.org/10.1038/s41598-023-31034-8>.

Correspondence and requests for materials should be addressed to B.P.

Reprints and permissions information is available at www.nature.com/reprints.

Publisher's note Springer Nature remains neutral with regard to jurisdictional claims in published maps and institutional affiliations.



Open Access This article is licensed under a Creative Commons Attribution 4.0 International License, which permits use, sharing, adaptation, distribution and reproduction in any medium or format, as long as you give appropriate credit to the original author(s) and the source, provide a link to the Creative Commons licence, and indicate if changes were made. The images or other third party material in this article are included in the article's Creative Commons licence, unless indicated otherwise in a credit line to the material. If material is not included in the article's Creative Commons licence and your intended use is not permitted by statutory regulation or exceeds the permitted use, you will need to obtain permission directly from the copyright holder. To view a copy of this licence, visit <http://creativecommons.org/licenses/by/4.0/>.

© The Author(s) 2023